FOREX Publication
Open Access | Rapid and quality publishing

International Journal of
Electrical and Electronics Research (IJEER)
Research Article | Volume 14, Issue 2 | Pages 436-445 | e-ISSN: 2347-470X

PQ-Constrained OLTC Optimization in EV-Integrated Distribution Systems Using Secretary Bird Optimization Algorithm

K. Ramamohana Reddy[1*], P. Ram Kishore Kumar Reddy[2], and P. Sujatha[3]

[1]Department of Electrical and Electronics Engineering, JNTUA University, Anantapuramu, India; Email: krammohanee@gmail.com
[2]Department of Electrical and Electronics Engineering, MGIT, Hyderabad, India
[3]Department of Electrical and Electronics Engineering, JNTUCEA, Anantapuramu, India

***Correspondence:** *K. Ramamohana Reddy, krammohanee@gmail.com*

ABSTRACT- The adoption of electric vehicles is increasing rapidly; this EV charging is most uncertain thing. The distribution system losses are high due to uncertain usage of power supply issues and it increases due to EV charging stations integration in the distribution side. This paper proposes the Secretary Bird Optimization Algorithm based optimal OLTC tap positions to minimize the power losses and improvement of voltage profile in the distribution system. In general, constant power loading is considered in distribution system but here in this proposed approach voltage dependent load modelling is adapted and integrated the various DG systems (both PV and wind), capacitor placement, to compensate the power losses before going to apply the OLTC as much as possible to reduce the power loss. The proposed approach is tested on IEEE 15 and IEEE 33 bus standard system and evaluated the proposed Secretary Bird Optimization Algorithm. Compared the proposed approach with existing algorithms like standard PSO algorithm, as well as compared with modern algorithms like PBO, GWO-MLP algorithms, Secretary Bird Optimization Algorithm outperformed and exhibits better loss reduction and improvement in voltage profile.

Keywords: Distribution Networks, Electric Vehicle Charging, On-Load Tap Changer (OLTC), Power Quality, Radial Feeders, Renewable Integration, Secretary Bird Optimization Algorithm (SBOA), Voltage-Dependent Load Modeling.

ARTICLE INFORMATION

Author(s): K. Ramamohana Reddy, P. Ram Kishore Kumar Reddy, and P. Sujatha;

Received: 13/11/25; **Accepted**: 21/04/26; **Published**: 25/06/26;
E- ISSN: 2347-470X;
Paper Id: IJEER 2101B07;
Citation: 10.37391/ijeer.140220
Webpage-link:
https://ijeer.forexjournal.co.in/archive/volume-14/ijeer-140220.html

Publisher's Note: FOREX Publication stays neutral with regard to jurisdictional claims in Published maps and institutional affiliations.

1. INTRODUCTION

Now-a-days the penetration of electric vehicles is increasing rapidly and due to this the EV charging behavior becomes highly uncertain in distribution systems. Unlike conventional loads, EV charging demand is concentrated and time varying, which creates sudden power demand at specific locations of the feeder. Along with this, rooftop and distribution-level renewable energy sources such as photovoltaic and wind systems are also increasing, which further disturbs the traditional operating assumptions of distribution networks. Bidirectional power flow and intermittent power generation may exacerbate the issues, such as maintaining an acceptable operating voltage and increasing loss.

The first disturbance to the voltage profile in distribution feeders is the addition of EV chargers. Fast, clustered EV chargers draw high current locally, severely lowering the voltage, especially at the end buses. PV DGs and wind based DGs are likely to feed power into the grid during high generation and can cause voltage rise. The bus voltages can potentially exceed the normal operating range of 0.9 to 1.1 pu if voltage rise is not addressed properly, and when the voltage drops, the current drawn from the system will go up. This leads to increased losses and heating of the equipment. In many works, constant power load models are used for analysis for the sake of simplicity. However, under realistic voltage variations of EVs and renewables, the loads are also voltage dependent, constant power models would produce unrealistic results. To obtain a more realistic assessment of power losses or the voltage profile, voltage dependent load modeling is necessary. To reduce the various losses such as power losses arising in the system, the capacitor placement is done, the PV systems are placed as DG to reduce real losses and the wind systems are placed to compensate the real and reactive power losses.

Proper placement and coordination of these devices can reduce losses and improve voltage profile to some extent. However, the on-load tap changer (OLTC) still plays a major role in controlling feeder-wide voltage levels. If OLTC operation is not properly coordinated with stochastic EV charging demand and renewable power variations, it may result in frequent tap operations, increased wear, and reduced effectiveness in voltage regulation. The optimal selection of OLTC tap

FOREX Publication
Open Access | Rapid and quality publishing
International Journal of Electrical and Electronics Research (IJEER)
Research Article | Volume 14, Issue 2 | Pages 436-445 | e-ISSN: 2347-470X

positions under such uncertain operating conditions becomes a nonlinear and complex optimization problem.

In this work, a staged approach is adopted for a radial distribution system with voltage dependent load modelling. Initially, the impact of EV charging on voltage profile and power losses is evaluated. Subsequently, distributed generation systems including PV and wind along with shunt capacitors are integrated to compensate for the losses as much as possible before applying OLTC control. Finally, optimal OLTC tap positions are determined using the Secretary Bird Optimization Algorithm considering stochastic power flow conditions. The proposed approach is tested on the IEEE 15-bus distribution system and the performance is evaluated in terms of power loss reduction and voltage profile improvement.

2. MATERIALS AND METHODS

Renewable energy resources are connected to reduce the pressure on the distribution feeders but rapid integration and uncertainty are still increasing the power losses. This EV charging stations integration leads to the voltage fluctuations and harmonics are introduced due to converters used in the DG systems integrations. This leads to increase the thermal stress and huge power losses, uneven voltage profiles in the distribution networks [1], [2].

In most of the earlier studies, constant power load assumption is considered in the analysis, which makes the problem simple but does not represent the actual operating conditions of the distribution system. When EV charging and renewable energy sources are integrated, the voltage at buses varies continuously and due to this the load demand also changes with respect to voltage. Because of this reason, voltage dependent load modeling is required to capture the practical behavior of residential, commercial, and industrial loads. ZIP and exponential load models are commonly used to represent this behavior, and by using these models, the estimation of power losses and voltage profile becomes more realistic under varying voltage conditions [3].

To reduce the PQ problems caused by EV charging and renewable integration, several compensation methods are reported in the literature. Reactive power support using PV and wind inverters, placement of shunt capacitors, and coordinated operation of OLTC are commonly adopted to control voltage variations. Along with this, smart charging strategies, vehicle-to-grid operation, and battery energy storage systems are also applied to reduce peak demand and voltage fluctuations. However, due to uncertainty in EV charging and renewable generation, harmonic mitigation and coordination of these devices still remain challenging in practical systems [4], [5]. To handle this uncertainty, metaheuristic-based optimization techniques are used to coordinate OLTC tap positions, inverter reactive power support, and compensation devices under varying operating conditions [6]–[8].

Recent investigations show that when voltage dependent load modeling is combined with coordinated control of distributed generation, energy storage systems, and OLTC, better voltage regulation and reduced power losses can be achieved. Simulation studies also indicate that proper coordination between inverter-based resources and OLTC is important in EV dominated feeders, especially when compensation devices are placed adaptively along the feeder [9]– [11]. Comparative analysis of optimization techniques such as PSO and other modern metaheuristic algorithms further indicate improvement in voltage stability and PQ indices in distribution systems with high EV and renewable penetration [12].

More recently, the Secretary Bird Optimization Algorithm (SBOA) has gained attention as a metaheuristic suited to complex, nonlinear optimization problems. Although applications in power systems remain limited, recent studies suggest strong potential for PQ enhancement, compensation allocation, and distribution system reconfiguration [13], [14].

Research Gaps Identified

- Existing studies rarely integrate PQ analysis, voltage-dependent load modeling, advanced compensation, OLTC control, and SBOA within a single optimization framework.
- Metaheuristic parameter tuning, computational burden, and scalability to large or real-time systems remain unresolved.
- The use of SBOA for PQ-oriented tap-setting problems in EV- and renewable-rich distribution networks is still limited, leaving clear scope for further investigation.
- Field-oriented studies are scarce, particularly those combining VDL models with coordinated device and OLTC control under high EV and RES penetration.

3. THEORY AND CALCULATION

The mathematical model of the electrical problem of the radial distribution feeder is based on load characteristics, the voltage dependency of the load, the demand for EV charging infrastructure and the distributed compensation (respectively PV, wind and shunt capacitors). A power-quality aware OLTC tap-setting optimization problem is defined using the mathematical model. The governing equations are stepwise developed starting from the feeder power flow equations, then including voltage sensitive load models, stochastic EV injections, and compensators. These terms are added into the composite optimization problem posed with a loss minimization objective, combined with regulated voltage quality management. This serves as the objective of a metaheuristic solution approach.

3.1. Distribution Network Representation

Consider a radial distribution feeder represented by a directed tree $\zeta = (\mathcal{N}, \varepsilon)$ where $\mathcal{N}$ is the set of buses and ε the set of branches. The slack bus is denoted by 0 and each branch $(i \rightarrow j) \in \varepsilon$ has series impedance.

FOREX Publication
Open Access | Rapid and quality publishing
International Journal of Electrical and Electronics Research (IJEER)
Research Article | Volume 14, Issue 2 | Pages 436-445 | e-ISSN: 2347-470X

$$z_{ij} = r_{ij} + jx_{ij}(pu) \quad (1)$$

Complex bus voltage and net complex power injection are $V_i \in \mathbb{C}$ *and* $S_i = P_i + jQ_i(pu)$. The load flow is solved using the Backward–Forward Sweep (BFS) method, where nodal and branch currents are expressed

$$I_i = \frac{\bar{S}_i}{V_i}, \;\; I_{ij} = \sum_{k\in\mathcal{D}(j)} I_k, \;\; V_j = V_i - z_{ij}I_{ij} \quad (2)$$

Where $\mathcal{D}(j)$ is the set of all loads downstream of j. Feeder real power loss is

$$P_{loss} = \sum_{(i\to j)\,\in\,\varepsilon} r_{ij}\,|I_{ij}|^2 S_{Base} \quad (3)$$

Equations (1)– (3) form the foundation of the distribution system model.

3.2.Voltage-Dependent Load Modelling

To realistically capture PQ dynamics, loads are modelled as voltage-sensitive rather than constant power. The active and reactive demands at bus i are given by

$$P_i(V_i) = P_i^{(0)}|V_i|^{\alpha_i^p}, \;\; Q_i(V_i) = Q_i^{(0)}|V_i|^{\alpha_i^q} \quad (4)$$

Where $P_i^{(0)}$ and $Q_i^{(0)}$ are nominal demands, and α_i^p, α_i^q are voltage exponents. This formulation ensures that load consumption dynamically follows voltage variations, thus influencing both losses and PQ indices.

3.3. Power Quality Indices

Two indices are employed to quantify PQ:

Voltage deviation index

$$VDI = \frac{1}{|\mathcal{N}|}\sum_{i\in\mathcal{N}}\big||V_i| - 1\big| \quad (5)$$

Violation Severity Score (VVS)

$$VVS = \sum_{i\in\mathcal{N}}[\max(0, 0.95 - |V_i|) + \max(0, |V_i| - 1.05)] \quad (6)$$

Equation (5) captures the average deviation from nominal voltage, while *eq. (6)* penalizes under- or over-voltage violations beyond IEEE 1159 limits.

3.4. EV Charging Model

Let $\varepsilon_{ev} \subset \mathcal{N}$ be EV buses with technology-dependent rated powers $P_i^{EV,base}$.

$$P_i^{EV}(V_i) = P_i^{EV,base}|V_i|^{\alpha_{EV}}, Q_i^{EV} = 0\,, \;\; i \in \varepsilon_{ev} \quad (7)$$

Where $P_i^{EV,base}$ is the rated EV charging power and α_{EV} reflects voltage sensitivity. This representation explicitly accounts for clustered, voltage-dependent EV demand.

3.5. Compensation Model

PV injections are modeled as negative loads (fractional offsets) with mild bounded stochasticity consistent with distribution-level variability

$$P_i \leftarrow P_i(1-\rho_i), \;\; \rho_i \in \{0.75, 0.25\} * \xi_i, \;\; \xi_i \in \{0.8, 1.0\} \quad (8)$$

Wind support is represented as multiplicative reductions on both P and Q at selected buses:

$$P_i \leftarrow P_i\big(1-\omega_i^p\big), Q_i \leftarrow Q_i\big(1-\omega_i^q\big), \omega_i^p = \omega_i^q = 0.5 \quad (9)$$

Capacitor banks provide shunt reactive injection that follows

$$Q_i \leftarrow Q_i - Q_i^{cap}(|V_i|), Q_i^{cap} = k_i|V_i|^2 \quad (10)$$

Equations (8)– (10) together represent distributed compensation mechanisms in the feeder.

3.6. OLTC Tap Model

The substation OLTC controls the slack bus voltage magnitude

$$|V_0| = t, \qquad t \in \mathcal{T} \quad (11)$$

Where $\mathcal{T}$ may be continuous [0.9, 1.1] or a discrete set of tap steps.

$$\mathcal{T} = \{t_{min}, t_{min} + \Delta, \ldots., t_{max}\}, \Delta = \frac{t_{max} - t_{min}}{N_{steps} - 1} \quad (12)$$

3.7. Composite Optimization Problem

The PQ-aware composite objective function is formulated as

$$\min_{t\in\mathcal{T}} J(t;\omega) = P_{loss}\,(t;\omega) + \alpha * VDI(t;\omega) + \beta * VVS(t;\omega) \quad (13)$$

Typical weights: $\alpha = O(10^1 \sim 10^2)$, $\beta \gg 1$ to strictly penalize PQ violations. Under stochastic RES and EV variability, the robust formulation is

$$\min_{t\in\mathcal{T}} \mathbb{E}_\omega[J(t;\omega)] \text{ s.t. } \mathbb{P}_\omega(0.9 \le |V_i(t;\omega)| \le 1.1, \forall i \ge 1 - \epsilon) \quad (14)$$

Equation (14) defines the PQ-constrained OLTC optimization problem.

3.8. Secretary Bird Optimization Algorithm (SBOA)

The optimization problem defined in *eq. (14)* is stochastic, non-convex, and derivative-free, and it includes both continuous and discrete decision variables through the OLTC tap settings. Gradient-based methods are not suitable because the objective relies on iterative power-flow calculations and non-differentiable penalty terms such as the violation severity score (VVS). For this reason, metaheuristic algorithms are more appropriate.

Among recent nature-inspired methods, the Secretary Bird Optimization Algorithm (SBOA) provides a balanced search strategy through two interacting phases: predation, which drives solutions toward the current best candidate, and escape, which promotes diversification and helps avoid local optima. This dual behavior allows SBOA to navigate complex search spaces effectively. The working principle of SBOA, including the predation–escape dynamics and the dual-proposal selection process, is illustrated in *figure 1*.

FOREX Publication
Open Access | Rapid and quality publishing
International Journal of Electrical and Electronics Research (IJEER)
Research Article | Volume 14, Issue 2 | Pages 436-445 | e-ISSN: 2347-470X

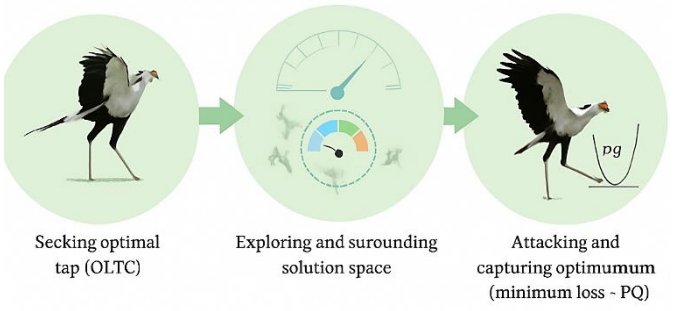

Figure 1. Conceptual illustration of the Secretary Bird Optimization Algorithm applied to OLTC tap setting, showing exploration of the solution space and convergence toward the optimal tap

SBOA operates on a population of candidate solutions (tap settings), denoted by $\{t_i^n\}_{i=1}^{N_P}$ at iteration n, with t^* representing the current global best.

3.8.1. Predation Phase

The predation phase mimics the hunting strategy of secretary birds, consisting of three regimes:

$$\tilde{t}_i^{(1)} = \begin{cases} t_i^{(n)} + r\left(t_a^{(n)} - t_b^{(n)}\right) & \text{(stalk: differential − type global step)} \\ t^* + \exp\left(\left(n/T\right)^4\right)(r_G - 0.5)\left(t^* - t_i^{(n)}\right) & \text{(approach: guided contraction)} \\ t^* + \phi(n) t_i^{(n)} * L & (attack: Levy\ flight, heavy - tailed\ jumps) \end{cases} \quad (15)$$

Where $r, r_G \sim \mathcal{U}(0,1), \phi(n) = (1 - n/T)^{\frac{2n}{T}}$, and L a Levy random variable (heavy-tailed) with stability parameter $\beta = 1.5$. The stalk step introduces diversity by combining two random particles. The approach step gradually contracts the population around the global best. The attack step leverages heavy-tailed Levy jumps to escape local minima.

3.8.2. Escape (two regimes)

The escape phase enables individuals to diversify when trapped by predators (local optima). Two update rules are used:

$$\tilde{t}_i^{(2)} = \begin{cases} t^* + \psi(n)(2r - 1) t_i^{(n)}, & hide: \text{controlled randomization} \\ t_i^{(n)} + r(t_k^{(n)} - K t_i^{(n)}), & fly/run: peer\ perturbation \end{cases} \quad (16)$$

where $\psi(n) = \left(1 - \frac{n}{T}\right)^{1 - \frac{n}{T}}, K \in \{1,2\}$ and $t_k^{(n)}$ is a randomly selected peer.

The hide step perturbs the particle relative to its own position. The fly/run step forces interaction with another solution, encouraging diversity.

3.8.3. Selection Mechanism

Both candidates $\tilde{t}_i^{(1)}$ (from predation) and $\tilde{t}_i^{(2)}$ (from escape) are evaluated using the PQ-aware objective function in *eq. (13)*. The better solution is retained:

$$t_i^{(n+1)} = \arg\min\left\{J\left(\tilde{t}_i^{(1)}\right), J\left(\tilde{t}_i^{(2)}\right)\right\} \quad (17)$$

If taps are discrete, the selected value is clamped/quantized into the admissible set $\mathcal{T}$.

This two-proposal selection is a key strength of SBOA, as it reduces the chance of incorrect promotion under stochastic evaluations by comparing candidates on the same scenario set.

3.8.4. Computational Complexity

For each iteration, the complexity is

$$\mathcal{O}\left(N_p * K * |\varepsilon|\right) \quad (18)$$

N_p is the population size, K the number of stochastic scenarios per evaluation, and $|\varepsilon|$ the number of branches (BFS complexity). Since all candidate evaluations are independent, SBOA is naturally parallelizable.

The procedural steps of the proposed SBOA-based OLTC optimization are summarized as follows:

Algorithm: SBOA-Based OLTC Optimization

Step 1: Initialize population of candidate tap settings within limits [0.9, 1.1]

Step 2: Evaluate objective function for each candidate using: Load flow analysis (BFS) and PQ indices (VDI, VVS)

Step 3: Identify initial global best and local best solutions.

Step 4: For each iteration (t = 1 to MaxIter)
Step 4.1: For each candidate solution
- Generate new solution using predation behavior
- Generate alternative solution using escape behavior
- Apply boundary constraints to maintain feasible tap range
- Evaluate both solutions using objective function
- Select the better solution

Step 4.2: Update local best and global best solutions
Step 4.3: Store convergence data (objective, loss, VDI)

Step 5: End iteration loop

Step 6: Return optimal tap setting and corresponding system performance

To show the applicability and the scalability of the proposed method, a set of two test cases is chosen. The first one is the IEEE 15-bus system which is used as a case study to show modeling of voltage dependent loads, integration of EVs and distributed compensation. Subsequently, the IEEE 33-bus radial distribution system is employed as the primary test system for validating the proposed SBOA-based OLTC optimization under realistic operating conditions and for performing statistical analysis.

The analysis is carried out on the IEEE 15-bus and IEEE 33 bus radial distribution systems and the simulation data are given in *table 1*. All loads are considered as voltage dependent and both active and reactive powers vary with bus voltage using nonlinear exponents. *Table 2* shows the different categories of loads like residential, commercial, industrial types.

FOREX Publication
Open Access | Rapid and quality publishing
International Journal of Electrical and Electronics Research (IJEER)
Research Article | Volume 14, Issue 2 | Pages 436-445 | e-ISSN: 2347-470X

Table 1. Simulation Parameters and System Configuration

Parameter	Value
Test System	IEEE 33-bus, IEEE 15-bus
Base Voltage	12.66 kV
Base Power	100 MVA
Load Model	Voltage-dependent
EV Locations	7, 14, 18, 25, 30, 33
PV Locations	6, 12, 18, 25, 31, 33
Wind Locations	10, 24, 30
Capacitors	15, 25, 30
Algorithm	SBOA
Population Size	50
Iterations	200
Runs	30
Decision Variable	OLTC Tap
Tap Range	0.9 – 1.1 pu
Objective Components	Loss + VDI + VVS

This setup maintains voltage dependent load behavior for residential, commercial, and industrial feeders. The bus-wise placement of distributed resources is given in Table 3. Photovoltaic systems are treated as stochastic active power reductions, where residential loads experience a maximum reduction of 25% and industrial loads up to 75%. Wind generation is modeled as a simultaneous reduction in active and reactive power, limited to 50%, with one industrial feeder allowed a higher active power reduction of 75%. Shunt capacitor banks are connected at buses 5 to 8 and inject reactive power based on the square of the local bus voltage. By combining PV, wind, and shunt capacitors, the compensation effect is distributed along the feeder and acts on both voltage variation and power loss before OLTC tap control is applied.

Table 2. Bus Load Categories and Voltage-Dependent Exponents

Bus No.	Load Type	αp	αq	Description
2–3	Commercial	0.18	6.00	Voltage-sensitive offices/shops
4	Commercial	0.18	6.00	Large commercial block
5–8	Industrial	1.51	3.40	Heavy industrial feeders
9–15	Residential	0.92	4.04	Mixed residential feeders

Table 3. Distributed Compensation (PV, Wind, Capacitors)

Bus No.	Technology	Maximum Reduction/Injection
5, 7	PV	Up to 75% load reduction (Rooftop PV industrial feeders)
9,10,12,14,15	PV	Up to 25% load reduction (Residential rooftop PV)
2	Wind	Up to 50% P & Q reduction (Small-scale wind DG)
4	Wind	Up to 50% P & Q reduction (Commercial-scale wind)
5	Wind	Up to 75% P reduction (Industrial feeder wind turbine)
5	Capacitor	30% Q injection
6	Capacitor	50% Q injection
7	Capacitor	50% Q injection
8	Capacitor	20% Q injection

The configuration of EV charging stations is summarized in *table 4*. AC Level-3, DC fast, and Level-2 chargers are placed across buses 3–15 to reflect clustered charging in commercial and residential feeders. Rated power ranges from 19.2 kW for residential Level-2 chargers to 200 kW for commercial DC Level-3 stations. Each charging station is modeled as an additional voltage-dependent load, capturing the power quality stress imposed by large, nonlinear charging demand.

Table 4. EV Charging Station Integration

Bus No.	EV Charger Type	Rated Power (kW)
3	AC Level-3	43.5
4	DC Level-3	200
6,7	DC Level-2	96 each
9,11,13,15	AC/DC Level-2	19.2 each

In this study, the IEEE 15-bus radial distribution system given in *tables (1)–(4)* is selected as the test network. All loads are modeled as voltage dependent so that the base case reflects real feeder behavior under voltage variation. On this base system, distributed resources such as photovoltaic systems, wind generators, and shunt capacitors are introduced to represent compensation. Different EV charging stations are added to increases uncertainty in feeder and makes voltage regulation and loss control more difficult. This combined setup forms the test environment for evaluating the Secretary Bird Optimization Algorithm in solving the OLTC tap-setting problem defined in *eq. (13)– (14)*. The proposed algorithm under test system examined in four stages as voltage load modelling, EV charging stations integrated, placement of DG, shunt capacitors, and finally OLTC tap with Secretary Bird Optimization Algorithm optimization, so that the contribution of each stage to power quality behavior can be identified clearly.

4. RESULTS

The results are analyzed in a stage-wise manner to understand how different factors affect the performance of the IEEE 15-bus radial distribution system. Initially, the analysis is carried out with voltage dependent load modeling, which represents the realistic behavior of the feeder under voltage variation. In the next stage, EV charging stations are integrated at selected buses and their impact on voltage profile and power losses is evaluated. In final stage applying the OLTC control using proposed algorithm and comparing the power losses and voltage profile with remaining stages.

FOREX Publication
Open Access | Rapid and quality publishing
International Journal of Electrical and Electronics Research (IJEER)
Research Article | Volume 14, Issue 2 | Pages 436-445 | e-ISSN: 2347-470X

Stage 1: Base Case

In this case voltage load modelling is applied to the test system, in this stage the feeder power losses are 56.06 kW and 44.50 kVAr, in term of apparent power loss of 71.57 KVA. *Fig. 2* shows the voltage profile of the distribution system, buses 13,14, and 15 shows the low voltage profile 0.951 pu, while the remaining buses maintains the voltage profile near to 1.0 pu. The voltage deviation index is 0.0373, which shows noticeable voltage variation across the feeder, although no voltage limit violations are observed and the violation severity score remains zero.

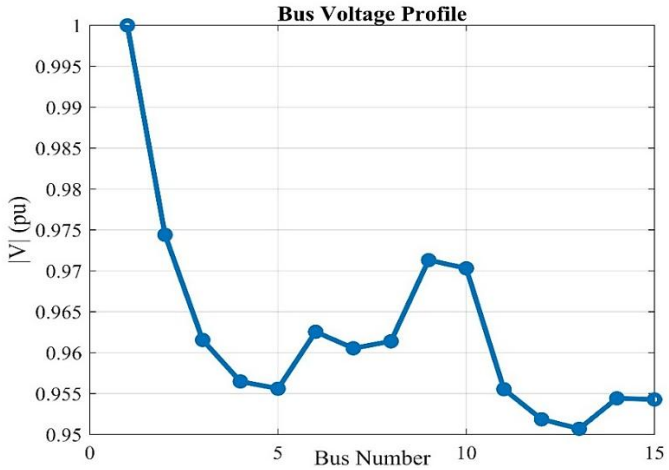

Figure 2. Distribution System Voltage Profile Under Voltage-Dependent Load Modelling

Commercial buses 2,3,4 (tables 1 and 2) exhibit higher voltage sensitivity due to large reactive power exponents (αq = 6.0), which leads to voltage drop in the middle section of the feeder. Industrial buses (5–8), with active and reactive voltage exponents of αp = 1.51 and αq = 3.40, draw higher demand when voltage reduces and thereby increase both active and reactive power losses. The residential buses (9–15), although having moderate voltage sensitivity (αp = 0.92, αq = 4.04), are distributed toward the tail end of the feeder and push the voltages close to the lower IEEE limit of 0.95 pu.

Stage 2: Impact of EV Charging Integration

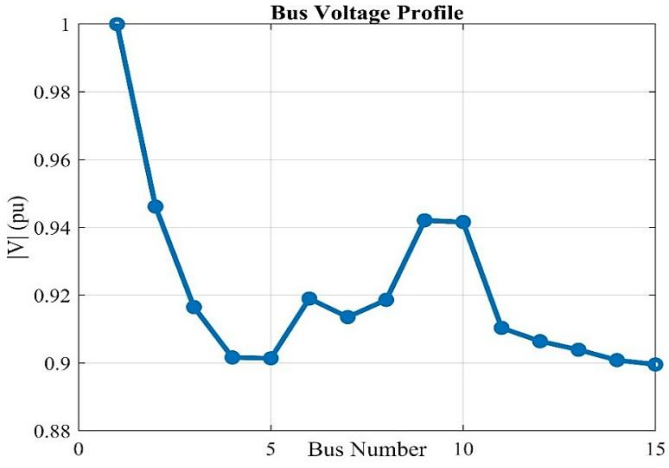

Figure 3. Impact of EV Charging Integration on Bus Voltage Profile

When compared with the base case, this clearly shows that clustered EV charging creates high loading on the distribution feeder. The voltage profile shown in *fig. 3* indicates voltage drop along the feeder, mainly at the middle and end buses. The minimum voltage reduces to 0.900 pu, while the substation side voltage remains close to 1.0 pu. The voltage deviation index increases to 0.0786 and one under-voltage condition is observed, which results in a nonzero violation severity score. Commercial buses with high reactive power sensitivity and fast charging show larger voltage reduction, and industrial and residential buses with multiple chargers maintain low voltage toward the feeder end. This stage indicates that EV charging without compensation increases losses and affects voltage profile, and therefore further compensation and OLTC control are required in the next stages.

Stage 3: Effect of Distributed Compensation

In Stage 3, distributed compensating resources are activated according to *table 3*. Rooftop PV systems are installed on residential buses 9, 10, 12, 14, and 15, providing up to 25% active power offset. Larger PV units on industrial feeders at buses 5 and 7 supply up to 75% offset. Small- to medium-scale wind generation is added at buses 2 and 4, and shunt capacitors are placed at buses 5–8, injecting 20–50% of local reactive power. This coordinated mix of active and reactive support illustrates the ability of hybrid compensation to counter the severe PQ degradation observed in Stage 2.

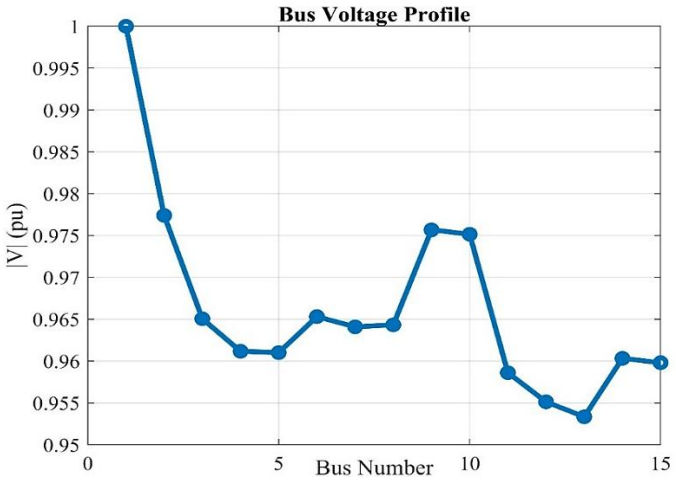

Figure 4. Effect of Distributed Compensation (PV, Wind, And Capacitors) on Bus Voltages

After applying distributed compensation, feeder losses reduce clearly. The real and reactive losses drop to 50.48 kW and 32.20 kVAr, resulting in an apparent loss of 59.88 kVA with an improved loss power factor of 0.84. When compared with the EV-only condition, this shows a large reduction in both active and reactive power losses. The voltage profile shown in *fig. 4* indicates recovery across the feeder, with the minimum bus voltage increasing to 0.953 pu. The voltage deviation index reduces to 0.0336, which is lower than the base case value. All bus voltages remain within the range of 0.9 to 1.1 pu and no voltage limit violations are observed. This stage indicates that distributed compensation reduces a major portion of the voltage variation and power losses created due to EV charging.

FOREX Publication
Open Access | Rapid and quality publishing
International Journal of Electrical and Electronics Research (IJEER)
Research Article | Volume 14, Issue 2 | Pages 436-445 | e-ISSN: 2347-470X

Still, under changing operating conditions, additional control is required to balance the feeder voltage and reduce losses, and for this OLTC tap optimization is applied in the next stage.

Stage 4: SBOA-Based OLTC Tap Optimization

In the final stage, the Secretary Bird Optimization Algorithm is used to adjust the OLTC tap position by changing the substation voltage within the allowed range. In the previous stages, the substation voltage is kept fixed, but in this stage the slack bus voltage is controlled to reduce feeder losses and voltage variation. The convergence of the Secretary Bird Optimization Algorithm is shown in *fig. 5*, where the objective value decreases step by step and settles at a stable value. The optimal tap ratio is obtained as 1.0125 pu, and the corresponding voltage profile is shown in *fig. 6*.

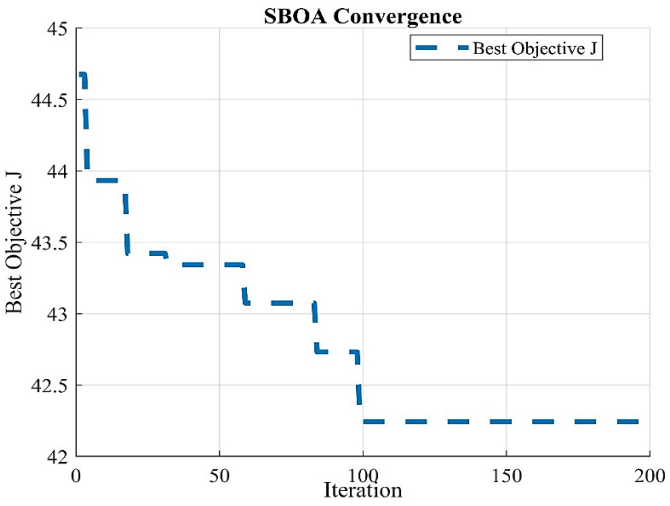

Figure 5. SBOA Convergence Characteristics Showing the Minimization of the PQ-Aware Objective Function

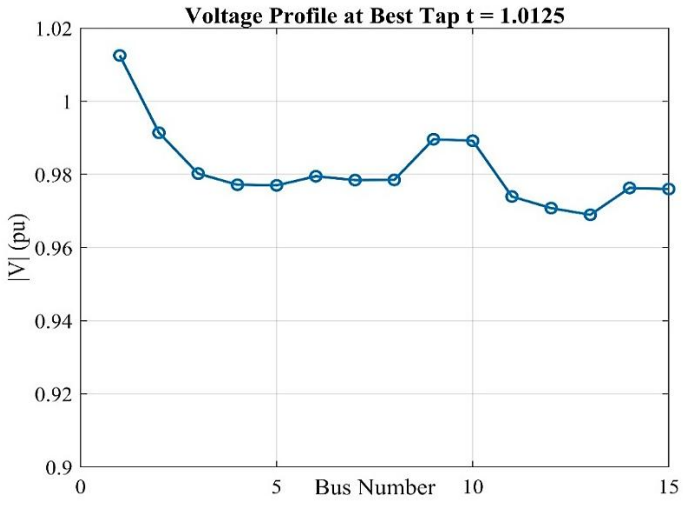

Figure 6. Optimized Voltage Profile using SBOA-Driven OLTC Tap Setting

By optimization of OLTC using proposed approach the distribution system voltage profile is flat response compared to remaining stages and voltage profile is improved, doesn't violated any limits.

The voltage deviation index reduces to 0.02036, which is the lower among all stages, and no voltage violations are observed. Feeder losses reduce further to 41.23 kW and 27.98 kVAr, resulting in an apparent loss of about 49.8 kVA. This reduction is clear when compared with the earlier stages, especially under EV charging conditions. This stage shows that OLTC tap optimization using SBOA further improves voltage profile and loss performance under EV and renewable uncertainty.

4.2. IEEE 33-Bus System: Validation and Statistical Analysis

To further validate the effectiveness and scalability of the proposed SBOA-based OLTC optimization framework, the analysis is extended to the IEEE 33-bus radial distribution system. Compared to the 15-bus system, the IEEE 33-bus feeder represents a more complex and practical distribution network with higher loading levels and deeper radial structure, making it suitable for evaluating the performance of the proposed method under realistic operating conditions.

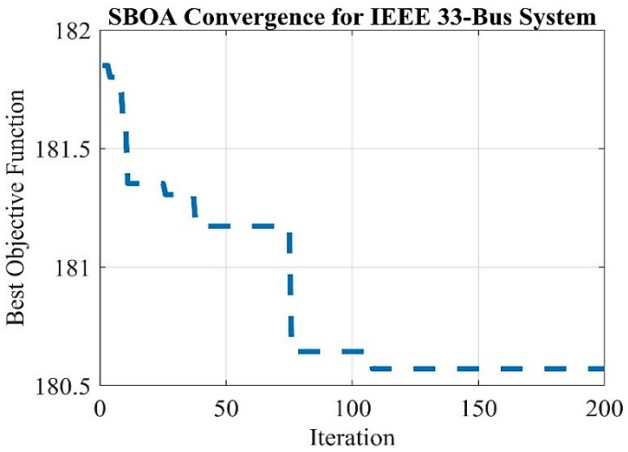

Figure 7. SBOA Convergence for IEEE 33 Bus System

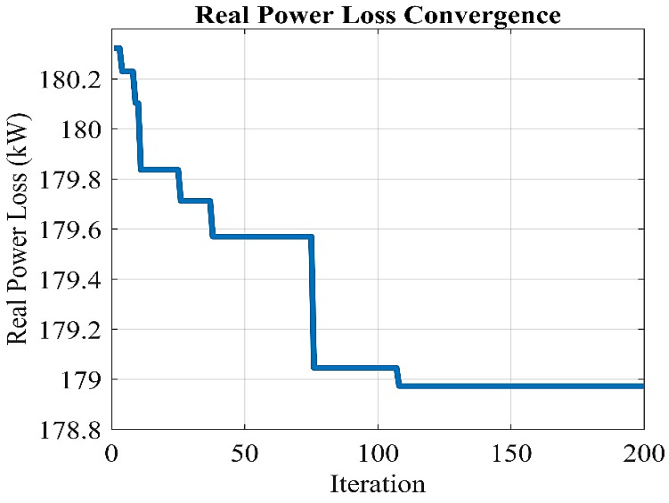

Figure 8. IEEE 33 Bus System Real Power Loss Reduction

To show the applicability and the scalability of the proposed method, a set of two test cases are chosen. The first one is the IEEE 15-bus test system used as a case study to show modeling of voltage dependent loads and the integration of

FOREX Publication
Open Access | Rapid and quality publishing
International Journal of Electrical and Electronics Research (IJEER)
Research Article | Volume 14, Issue 2 | Pages 436-445 | e-ISSN: 2347-470X

EVs and distributed compensation. *Fig. 7* shows the convergence characteristics of SBOA, the objective function value minimized slowly by iterations and stabilized.

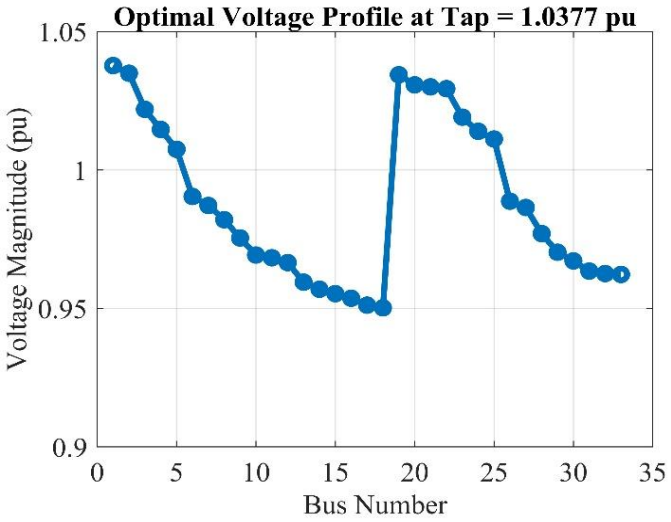

Figure 9. IEEE 33 Bus System Voltage Profile

Ultimately, as shown in *fig. 8*, the real power loss converges and the feeder losses decrease. The voltage profile of the IEEE 33-bus system with optimal tap settings is shown in *fig. 9*, which guarantees that all bus voltages are within the permissible range.

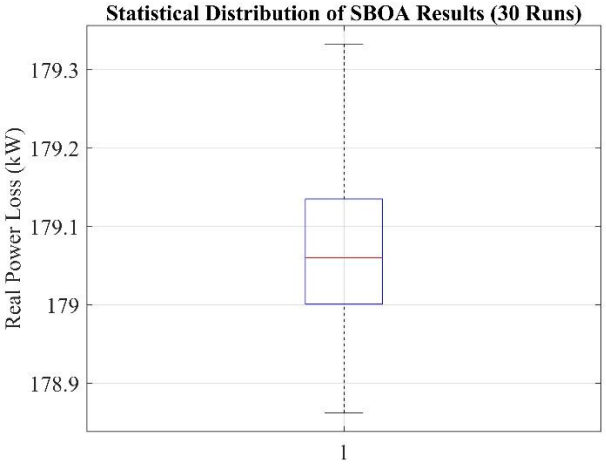

Figure 10. Statistical Distribution of Real Power Loss for IEEE 33-Bus System (30 Runs)

Fig. 10 presents the statistical distribution of real power loss over 30 independent runs, illustrating the consistency and robustness of the proposed SBOA-based optimization.

5. DISCUSSION

Table 5 shows the performance of the IEEE 15-bus distribution system at different stages. In the base case, the system already shows some voltage variation due to radial structure and voltage dependent loads. The minimum voltage is observed as 0.951 pu and the voltage deviation index is 0.0373. Even without EV charging, the feeder shows noticeable voltage drop and power loss.

Table 5. Comparative Performance of the IEEE-15 Bus Feeder Across Stages

Stage	Tap (P.U.)	Apparent Loss (kVA)	Loss PF	Vmin / Vmax	VDI	VVS	Violations (Under/ Over)
1	1.0000	71.57	0.7832	0.951 / 1.000	0.03728	0.00000	0 / 0
2	1.0000	501.66	0.7300	0.900 / 1.000	0.07858	0.00047	1 / 0
3	1.0000	59.88	0.8431	0.953 / 1.000	0.03358	0.00000	0 / 0
4	1.0125	49.82	0.8300*	0.969 / 1.013	0.02036	0.00000	0 / 0

Upon adding EV charging stations in Stage 2, the feeder losses are calculated to be: real power loss = 366.2 kW, reactive power loss = 342.8 kVAr and apparent power loss = 501.7 kVA. A minimum bus voltage of 0.90 pu and one under-voltage case are stated, indicating that on a feeder, clustered EV charging can affect not only energy losses, but also its voltage profile.

In Stage 3, the addition of PV systems, wind generators and shunt capacitors provide further compensation, reducing the voltage deviation index from 0.0970 to 0.0336 and the system losses. The voltage deviation index reduces to 0.0336 and no voltage violations are observed. The power losses reduce to 50.5 kW and 32.2 kVAr. This indicates that local compensation reduces the effect of EV charging on feeder voltage and losses. In Stage 4, OLTC tap control is applied using the Secretary Bird Optimization Algorithm. With the tap value adjusted to 1.0125 pu, the voltage levels along the feeder remain closer to each other. All bus voltages remain within the range of 0.969 to 1.013 pu. The voltage deviation index further reduces to 0.0204 and feeder losses reduce to 41.2 kW and 27.9 kVAr. This stage shows that OLTC tap control further improves voltage profile and loss performance when EV charging and distributed generation are present.

Table 6. Comparative Performance of the IEEE-33 Bus Feeder Across Stages

Stage	Tap (p.u.)	Apparent Loss (kVA)	Loss PF	Vmin / Vmax (p.u.)	VDI	VVS	Violation (Under/ Over)
1 (Base Load)	1.0000	248.6	0.82	0.913 / 1.000	0.0821	0.412	6 / 0
2 (+ EV)	1.0000	276.3	0.81	0.895 / 1.000	0.0954	0.785	9 / 0
3 (+ DG + Capacitor)	1.0000	232.8	0.83	0.938 / 1.000	0.0587	0.112	2 / 0
4 (+ OLTC - SBOA)	1.0375	215.7	0.83	0.9501 / 1.0375	0.0318	0.000	0 / 0

FOREX Publication
Open Access | Rapid and quality publishing
International Journal of Electrical and Electronics Research (IJEER)
Research Article | Volume 14, Issue 2 | Pages 436-445 | e-ISSN: 2347-470X

Table 7. Statistical Performance of SBOA (IEEE 33-Bus System)

Metric	Value
Best Loss (kW)	178.8235
Mean Loss (kW)	179.0714
Worst Loss (kW)	179.4824
Standard Deviation (kW)	0.1409

This stage shows that OLTC tap control further improves voltage profile and loss performance when EV charging and distributed generation are present. The performance of the proposed method on the IEEE 33-bus system is summarized in *table 6*, Comparative Performance of the IEEE-33 Bus Feeder Across Stages.

The robustness of the proposed SBOA-based OLTC optimization framework was evaluated through 30 independent simulation runs under stochastic EV charging and renewable generation conditions. The statistical results are summarized in *table 7*. The algorithm achieved a minimum real power loss of 178.8235 kW, with an average loss of 179.0714 kW across all runs. The standard deviation was observed to be 0.1409 kW, indicating highly consistent convergence behavior.

Table 8. Comparative Performance of OLTC Tap Optimization Approaches

Methodology	Real Power Loss (kW)	Reactive Power Loss (kVAr)	Transformer Tapping (PU)
Base Case	56.06	44.50	1.0000
PSO [15]	44.12	32.53	0.9820
PBO [16]	46.53	30.65	0.9276
GWO–MLP	48.04	30.42	0.9010
SBOA (Proposed)	41.23	27.98	1.0125

Table 8 compares the proposed SBOA based OLTC method with other optimization techniques. PSO [6] and PBO [13] reduce losses but the tap positions remain below nominal values. The GWO–MLP method requires a lower tap setting, which may increase stress on downstream buses. The SBOA based method achieves lower losses while maintaining a near nominal tap position. This helps in keeping voltage within limits and reducing feeder losses under uncertain EV charging conditions.

6. CONCLUSION

A numerical study has been carried out in stages to understand the effects of EV charging and renewable energy in a radial distribution system. The study starts with a voltage dependent load, and successively incorporates EV charging, distributed generation, and OLTC control. It is easy to see how each input affects the system behavior in terms of both voltage profile and power losses. This means uncoordinated EV charging increases the stress on the feeder. In addition, both real power and reactive power losses increase, and several buses' voltages move closer to the lower limit of their particular allowable voltage range. This confirms that EVs without control can cause severe operational issues in distribution systems. The voltage profile as well as the losses of the system could be improved with the inclusion of the PV systems, the wind generators and the shunt capacitors. But due to the position and the working of these devices, this improvement is not enough for all situations. Some improvements are made using the tap control of OLTC, which is guided by the Secretary Bird Optimization Algorithm. The voltage profile is more balanced across the feeder and there are no voltage violations at the buses. For the power system of IEEE 33-bus, the optimal tap is around 1.0375 pu. This maintains the same operating point but reduces losses. To verify the reliability, the result of the optimization process is repeated 30 times using independent runs. The results show very small variation in power loss, indicating that the algorithm performs consistently even under changing EV and renewable conditions. The comparison with other methods such as PSO, PBO, and GWO–MLP shows that the proposed SBOA approach achieves lower losses while keeping the tap settings close to nominal values. This helps in avoiding unnecessary tap movements and improves voltage stability. The proposed framework demonstrates consistent performance and scalability, making it suitable for practical distribution system applications under EV and renewable uncertainty.

Funding Source: "This research received no external funding"

Conflicts of Interest: "The authors declare no conflict of interest."

REFERENCES

[1] Ibrahim, R.A., Gaber, I.M. & Zakzouk, N.E. Analysis of multidimensional impacts of electric vehicles penetration in distribution networks. Sci Rep 14, 27854 (2024). https://doi.org/10.1038/s41598-024-77662-6.

[2] Etanya, Tiku Fidelis, Pierre Tsafack, and Divine Khan Ngwashi. "Grid-connected distributed renewable energy generation systems: Power quality issues, and mitigation techniques–A review." Energy Reports 13 (2025): 3181-3203.

[3] A. Parker, M. A. Alkrch, K. James, A. Almaghrebi and M. A. Alahmad, "Framework to Develop Time- and Voltage-Dependent Building Load Profiles Using Polynomial Load Models," in IEEE Access, vol. 9, pp. 128328-128344, 2021, doi: 10.1109/ACCESS.2021.3112937.

[4] Barman, Pranjal, Lachit Dutta, Sushanta Bordoloi, Anamika Kalita, Pronamika Buragohain, Swapna Bharali, and Brian Azzopardi. "Renewable energy integration with electric vehicle technology: A review of the existing smart charging approaches." Renewable and Sustainable Energy Reviews 183 (2023): 113518.

[5] Nandini, K. K., and N. S. Jayalakshmi. "A combined approach to evaluate power quality and grid dependency by solar photovoltaic based electric vehicle charging station using hybrid optimization." Journal of Energy Storage 84 (2024): 110967.

[6] Venkatesan, R., C. Kumar, C. R. Balamurugan, and Tomonobu Senjyu. "Enhancing power quality in grid-connected hybrid renewable energy systems using UPQC and optimized O-FOPID." Frontiers in Energy Research 12 (2024): 1425412.

[7] Gholami, Khalil, Md Rabiul Islam, Md Moktadir Rahman, Ali Azizivahed, and Afef Fekih. "State-of-the-art technologies for volt-var control to support the penetration of renewable energy into the smart distribution grids." Energy Reports 8 (2022): 8630-8651.

International Journal of
Electrical and Electronics Research (IJEER)
Research Article | Volume 14, Issue 2 | Pages 436-445 | e-ISSN: 2347-470X

[8] Murray, William, Marco Adonis, and Atanda Raji. "Voltage control in future electrical distribution networks." Renewable and sustainable energy reviews 146 (2021): 111100.

[9] Tamhankar, Manjiri Mayuresh, and Ramchandra Pandurang Hasabe. "Efficient power management for sustainable EV charging station in DC microgrids." Journal of Integrated Science and Technology 13, no. 6 (2025): 1131-1131.

[10] Kumar, G. Naveen. "Characterizing Voltage-Dependent Loads and Frequency-Dependent Loads for Load Stability Analysis." In Smart Buildings Digitalization, pp. 207-216. CRC Press, 2022.

[11] Gholami, Khalil, Md Rabiul Islam, Md Moktadir Rahman, Ali Azizivahed, and Afef Fekih. "State-of-the-art technologies for volt-var control to support the penetration of renewable energy into the smart distribution grids." Energy Reports 8 (2022): 8630-8651.

[12] Mousa, Yasmin GH, Tarek S. Abdelsalam, Hany M. Hasanien, Zia Ullah, Abdulaziz Alkuhayli, and Mohamed Mokhtar. "Comparative analysis of metaheuristic algorithms-based control for enhancing low voltage ride through in grid-connected photovoltaic systems." Ain Shams Engineering Journal 16, no. 7 (2025): 103423.

[13] Zhu, Yu, Mingxu Zhang, Qinchuan Huang, Xianbo Wu, Li Wan, and Ju Huang. "Secretary bird optimization algorithm based on quantum computing and multiple strategies improvement for KELM diabetes classification." Scientific Reports 15, no. 1 (2025): 3774.

[14] Wang, Xinle, Peijun Wei, and Yancang Li. "Enhanced secretary bird optimization algorithm with multi-strategy fusion and Cauchy–Gaussian crossover." Scientific Reports 15, no. 1 (2025): 23163.

[15] Srinivas, C., Kranthi Kumar, I., Prasad Pandalaneni, N.D.V., Madhusudhan Reddy, N., “Minimization of Power Loss in Distribution System by Tap Changing Transformer using PSO Algorithm”, International Journal of Electrical and Electronics Research, 2022, 10(4), pp. 1135–1139, https://doi.org/10.37391/IJEER.100460.

[16] Reddy, M. Rama Prasad, Chodagam Srinivas, Bireddi Eswararao, Rajendraprasad Kuriti, and M. Koteswara Rao. "Addressing Power Loss and Voltage Profile Issues in Electrical Distribution Systems: A Novel Approach Using Polar Bear Gradient-Based Optimization." International Journal of Electrical and Electronics Research 11, no. 3 (2023): 788-793.